ON-ORBIT APPLICATION OF H-INFINITY TO THE MIDDECK ACTIVE CONTROLS EXPERIMENT: OVERVIEW OF RESULTS

Jessica A. Woods-Vedeler[*] and Lucas G. Horta[†]

The Middeck Active Control Experiment (MACE) was successfully completed during the flight of STS-67 in March 1995. MACE provided an on-orbit validation of modern robust control theory and system identification techniques through the testing of a flexible, multi-instrument, science platform in the micro-gravity environment of the Space Shuttle's Middeck. As part of this experiment, H-infinity control design was validated in zero gravity (0-G) environment. The control objective was to isolate a payload sensor from a 50Hz bandwidth disturbance occurring on the test article. Controllers were designed with the use of finite element models developed using 1-G measurements and a measurement model obtained by applying system identification techniques to open loop data obtained on orbit. Over 50 single-input, single-output and multi-input, multi-output, single and multi-axis H-infinity control designs were evaluated on-orbit. Up to 19 dB reduction in vibration levels and 25 Hz bandwidth of control were achieved.

INTRODUCTION AND BACKGROUND

The Middeck Active Control Experiment (MACE) was successfully completed during Space Shuttle flight STS-67 in March 1995. MACE provided an on-orbit validation of modern robust control theory and system identification techniques through the testing of a flexible, multi-instrument, science platform in the micro-gravity environment of the Space Shuttle's Middeck. Participants in the program were NASA Langley Research Center, MIT's Space Engineering Research Center, and Payload Systems, Inc (PSI).

MACE represents the first experimental validation of modern robust control design and dynamics modeling techniques in the zero-gravity (0-G) environment. Robust disturbance rejection, pointing and scanning were all achieved by the MACE Science Team using control system designs based on Finite Element models developed and validated in the 1-G and extrapolated to the 0-G environment. Control systems were also evaluated which were designed with measurement models developed using system identification techniques applied to data obtained on orbit.

The objective of this work was to apply the H-infinity control design methodology to the development of robust control systems for payload vibration isolation on the Middeck Active Controls Experiment (MACE). Although many varied types of experiments have been conducted to validate the theory[1,2], this paper describes the first known use of it in the 0-G environment. This technology demonstration is an important step in gaining acceptance of H-infinity and other advanced control methodologies for space based applications.

[*]Aerospace Engineer, Structural Dynamics Branch, NASA Langley Research Center, Hampton, VA 23681
[†]Assistant Branch Head, Structural Dynamics Branch, NASA Langley Research Center, Hampton, VA 23681

The paper describes results obtained from the on-orbit experimental validation of control systems designed using the H-infinity methodology. Discussion begins by describing the MACE experimental hardware and test procedure. A description of the design objective and the H-infinity design procedure follows. Detailed in these sections are the type of controllers developed for the experiment and the analysis used. Finally, results of the experiment are summarized.

DESCRIPTION OF EXPERIMENTAL HARDWARE

The MACE test article, shown in Figure 1, was about 1.7 meters long, weighed approximately 39 kg and was instrumented with multiple actuators and sensors. The bus structure was composed of circular cross-section Lexan struts connected by aluminum nodes. At each end of the flexible bus, a two-axis direct drive gimbal assembly was mounted. The gimbal assemblies acted as the payload at one end of the bus and as a multi-axis disturbance source at the other. Each gimbal assembly was instrumented with two-axis rate gyros and optical angle encoders to measure gimbal rotation. At the bus center, a three-axis reaction wheel assembly was mounted and instrumented with rate gyros. These reaction wheels were mounted at skewed angles but could be commanded in unison to actuate in the X-Y-Z axes directions. The test article was also instrumented with strain gauges and an active strut. In addition, two configurations of the test article were tested. Configuration 1 was as shown in Figure 1. For configuration 2, the bus structure was changed by rotating the primary payload strut, labeled BC in Figure 1, in the +Y direction, making it perpendicular to the bus axis at the node labeled B.

Control designs were implemented on MACE using real-time computer with a sampling rate of 500 Hz. The real time computer was capable of handling up to 20 sensors, 9 actuators, and an 80 state compensator. Total time delay from filters, sensors, computations and zero-order holds was about 11 milliseconds.
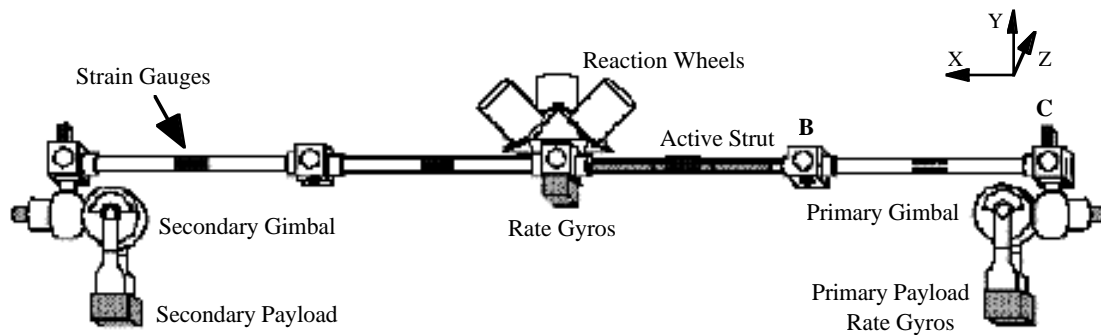

Figure 1 Middeck Active Controls Experiment (MACE) hardware sketch.

During the mission, data storage and crew interface functions were provided by the Experimental Support Module (ESM). Data up-link and down-link capabilities between the shuttle astronauts and the MACE Science Team were provided during the mission by a PSI developed Ku-Band Interface System (KIS) which had a capacity of 40MB per event.

EXPERIMENTAL PROCEDURE

The general procedure for testing control designs was as follows. Before the STS-67 mission, several protocols were designed based on finite element model (FEM) predictions of the 0-G dynamics. These designs were stored on the MACE flight computer before launch and experimentally evaluated on the test hardware when in orbit. A subset of test results obtained was then downlinked by astronauts from the Space Shuttle to researchers on the ground at JSC's Mission Control Center via KIS. Also downlinked during the first day of testing were open loop transfer functions of the test article in the Middeck's 0-G environment. Based on the limited controller performance information and the new models developed using system identification techniques on the open loop data, control systems were redesigned and uplinked to the shuttle for experimental evaluation. In this way, it was possible to update control designs four times.

MACE DESIGN OBJECTIVE

The H-infinity control objective was to isolate the payload rate gyro platform from a 50 Hz bandwidth white noise disturbance input applied by the secondary payload gimbals.

Several sensor and actuator combinations were of interest for each of the two hardware configurations. These combinations are summarized in Table 1. The first case investigated was single axis control in the X and Z directions using single-input, single-output (SISO) control. This case used the primary gimbal at the payload location as an actuator and the collocated rate gyro as a sensor. The disturbance was introduced into the system using the appropriate X or Z axis secondary payload gimbal. SISO control was also investigated with single axis actuation from the reaction wheels and single axis rate feedback from the collocated rate gyros. In addition, multi-input, multi-output (MIMO) control was also of interest. For single-axis control, a primary gimbal at the payload location was coupled with single axis reaction wheel actuation at the bus center. Collocated rate gyro sensor data at both locations was used as feedback. Finally, multi-axis control was investigated using X and Z axis primary gimbal actuation simultaneously with feedback from collocated X and Z axis rate gyros. In this multi-axis case, the disturbance was introduced by using the X and Z axis secondary payload gimbals simultaneously.

Table 1
ACTUATOR/SENSOR COMBINATIONS EVALUATED

X Axis Control
    Payload Gimbal X and Payload Rate Gyro X
    Reaction Wheel X and Bus Rate Gyro X
    Payload Gimbal X and Reaction Wheel X with Payload and Bus Rate GyrosX

XY Axis Control
    Payload Gimbal X and Reaction Wheels X and Y
       with Payload Rate Gyro X and Bus Rate Gyros X and Y

Z Axis Control
    Payload Gimbal Z and Payload Rate Gyro Z
    Reaction Wheel Z and Bus Rate Gyro Z
    Payload Gimbal Z and Reaction Wheel Z with Payload and Bus Rate Gyros Z

XZ Axis Control
    Payload Gimbals X and Z with Payload Rate Gyros X and Z

* Reaction Wheels 1, 2 and 3 are used in combination to actuate in the X, Y and
Z directions. Similarly, Bus Rate Gyros 1, 2 and 3 are resolved into the X, Y
and Z directions for control feedback.

H-INFINITY DESIGN PROCEDURE

The procedure used to design H-infinity controllers for the MACE experiment is presented in this section. Within this discussion is an overview of the H-infinity theory. Reference 3 is recommended for a more detailed discussion of the theory.

Model Order Reduction

For the MACE experiment, several dynamics models of the test article were available. The first, and primary, model used for design work was a 0-G finite element model (FEM). This model was developed and validated using data from a laboratory model under gravity and extrapolated to the 0-G environment.[4] The second model was an identified model developed using data obtained on-orbit and downlinked to the MACE Science Team during the mission.[5] FEM and Measurement Models (MM) were available for both configurations. Because these models had 130-150 states, model reduction was necessary for control design and was performed using a balanced model reduction technique.[6]

Weighting Functions and Uncertainties

In the H-infinity framework, robustness and performance requirements are specified using weighting functions and uncertainties. Figure 2 shows a block diagram representation of a system with the weighting and uncertainty functions included. In the block diagram, P is the

plant dynamics, K is the controller, $\Delta's$ represent uncertainties and W's are frequency dependent weighting functions. Four types of uncertainties are illustrated. First is a multiplicative uncertainty at the plant input, Δ_{r1}. This type of uncertainty specification is used to represent modeshape errors and actuator uncertainties. A multiplicative uncertainty at the plant output, Δ_n, can be used to describe measurement noise and sensor uncertainty. Additive plant uncertainty, Δ_{r2}, is used when unmodelled high frequency dynamics are present and to help produce a smooth transition between controlled and uncontrolled systems when the controller rolls off in regions where modes are present.[2] In each case, W represents a frequency dependent weighting function which describes the amount of robustness required. The requirement is a function of the noise level present or the anticipated amount of modal uncertainty. Performance may also be specified as an uncertainty according to the particular problem under study. For this particular case, performance is shown as a perturbation to the disturbance at the plant input, Δ_p, with the objective of minimizing the effect of the perturbation in the plant output. The performance weighting function represents the inverse of the amount of disturbance attenuation required.
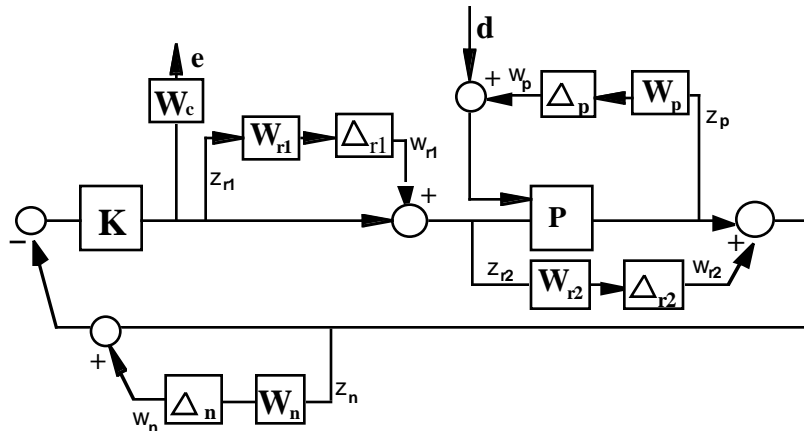

Figure 2 General H-infinity design structure showing uncertainties and weighting functions.

MACE control designs included several combinations of additive uncertainty, multiplicative output uncertainty and control weighting. In order to maximize performance, multiplicative uncertainty at the plant input was not used. A previous study[7] has shown that H-infinity produces controllers which achieve higher robustness levels than that which would be guaranteed in an optimal H-infinity design which included a multiplicative input type modal robustness specification. The implication of achieving high robustness levels is reduced performance level. Therefore, it was decided to take advantage of H-infinity's inherent robustness (ie. conservatism) to maximize potential performance by not specifying modal uncertainty as a multiplicative input. Unfortunately, this limits the capability to affect

robustness violations which arise due to modal uncertainty. Therefore, local robustness problems which arose were treated using notches in the control weighting function to simply prevent large actuation at specific frequencies.

H-infinity Control Design

The weighting functions are augmented to the plant matrix, P, and a linear fractional transformation is defined through block diagram manipulation of Figure 2. In Figure 3, this augmented plant matrix representation of the open loop dynamics is represented by the transfer function T. The inputs to T are W, which is a vector of the perturbation inputs, w_r, w_p, and w_n; d, which is an externally applied disturbance; and u, which is the control input. The outputs to T are z_y, which are the performance variables; Z, which is a vector of the perturbation outputs z_r, z_p, and z_n; and y, which is the control feedback. Inclusion of the controller, K, into T defines the linear fractional transformation, $F_l(P,K)$.
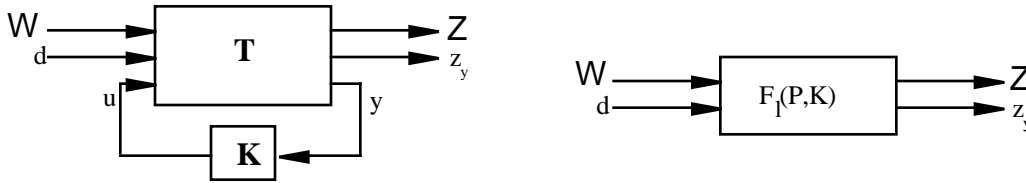

Figure 3 Linear fractional transformation of augmented plant matrix.

The H-infinity design methodology is then applied to the augmented plant matrix. The objective of the design optimization is minimize the H-infinity norm of $F_l(P,K)$ over controllers, K, such that

$$\left\| F_l(P,K) \right\|_\infty < \gamma$$

where $\gamma = 1$ for an optimal design and where it is assumed that uncertainties are unstructured, stable perturbations with $\left\| \Delta \right\|_\infty < 1$.

The H-infinity norm is defined as

$$\left\| F_l \right\|_\infty = \sup_\omega \left| F_l(j\omega) \right|$$

for SISO systems and

$$\left\| F_l \right\|_\infty = \sup_\omega \bar{\sigma}\left[F_l(j\omega) \right]$$

for MIMO systems, where $\bar{\sigma}$ indicates the maximum singular value of the transfer function and is a function of frequency.

Design Analysis

Once K is determined, stability must be evaluated. Although stability of the closed loop system is guaranteed on the reduced order design model by the H-infinity design methodology,

6

stability of the closed loop system must be evaluated on the full order model and with open loop experimental test data, if available.

Multivariable Nichols plot is used to determine absolute stability. The Nichols plot is defined using the magnitude of the following equation

$$N(s) = \det(I + PK) - 1$$

where P is the unaugmented plant and K is the controller. In the SISO case, the Nichols plot may also be used to indicate relative stability. Closed loop sensitivity may also be considered and must satisfy the condition

$$\bar{\sigma}\left[(I + PK)^{-1}\right] < 1$$

where $\bar{\sigma}$ indicates the maximum singular value of the transfer function and is a function of frequency.

Meeting robustness and performance criteria are key issues and the H-infinity design must be evaluated to determine how well each is met. Nominal performance is achieved if

$$\left\| F_l(P,K)_{w_p, z_p} \right\|_\infty \leq 1$$

where subscripts indicate a transfer function between specified inputs and outputs of $F_l(P,K)$. Robust stability is achieved if

$$\left\| F_l(P,K)_{\left[w_r\, w_n\right], \left[z_r\, z_n\right]} \right\|_\infty \leq 1$$

and if the closed loop system is internally stable in the presence of uncertainties. However, nominal performance and robust stability do not necessarily indicate the combined "robust performance" in which performance and robustness criteria are met simultaneously. The robust performance criteria is met when

$$\left\| F_l(P,K)_{\left[w_r\, w_n\, w_p\right], \left[z_r\, z_n\, z_p\right]} \right\|_\infty \leq 1$$

and if the closed loop system is internally stable in the presence of uncertainties.

There is an implicit assumption for a general, unstructured type uncertainty. However, a less conservative evaluation of robust performance can be made using structured uncertainties. In this case, for robust performance,

$$\left\| F_l(P,K)_{\left[w_r\, w_n\, w_p\right], \left[z_r\, z_n\, z_p\right]} \right\|_\mu \leq \left\| F_l(P,K)_{\left[w_r\, w_n\, w_p\right], \left[z_r\, z_n\, z_p\right]} \right\|_\infty \leq 1$$

where μ represents the structured singular value. In this study, both unstructured and complex diagonal structured uncertainties were considered.

Performance Criteria

Designs were compared on the basis of an H_2 performance index given by the state cost function

$$J = \int_{-\infty}^{+\infty} tr\left[G_{cl}^*(j\omega)R_{xx}G_{cl}(j\omega)\right]d\omega$$

where x are the states of the system, G_{cl} is the closed loop transfer function, Rxx is a state weighting matrix and * indicates a complex conjugate transpose. Although the H-infinity methodology minimizes a frequency domain norm, the H_2 norm was used to provide a relatively consistent means of comparison among all the various control methodologies evaluated during the experiment. The performance for each design is specified as

$$\Delta J = J_{cl} - J_{ol}$$

where the subscripts *cl* and *ol* indicate closed loop and open loop performance, respectively.

RESULTS

A variety of control configurations were tested. A summary of the actuator and sensor combinations evaluated for both hardware configurations was given in Table 1. SISO X and Z axis control designs were successfully tested on-orbit for both hardware Configurations 1 and 2. MIMO XZ axis control designs were also successfully tested. MIMO designs for Z axis control demonstrated limited success, while MIMO X and XY axis control designs were not successful.

SISO Control Design for Configuration 1

Figures 4 through 13 show some results from analysis and testing for SISO control designs. In each bar chart, a comparison is made between performance predicted on analytical models, performance predicted on the open loop experimental data and the actual performance obtained during testing. The analytical performance indicated is with respect to either the FEM or the Measurement Model (MM), depending on which model was used for control design. The vertical axis represents dB reduction in terms of the state cost function defined above. In the transfer function figures, the open loop disturbance transfer function is shown in comparison to the closed loop disturbance transfer function to show actual attenuation of disturbance levels.

Figure 4 illustrates a comparison of SISO X axis control results using Configuration 1. There were four designs which used the primary X axis gimbal as actuator and the payload X axis rate gyro as sensor. For each of the designs, the performance specification was 80% reduction in disturbance levels; robustness to 5% modal uncertainty at low frequencies and 10% at high frequencies; and robustness to noise levels at 5%. Design 2 is a reduced order

8

version of Design 1, Design 4 is a reevaluation of Design 1, and Design 3 is Design 1 without notch filters in the control weighting function. For evaluation of each design, the secondary X axis gimbal was used to introduce a 50 Hz bandwidth disturbance.
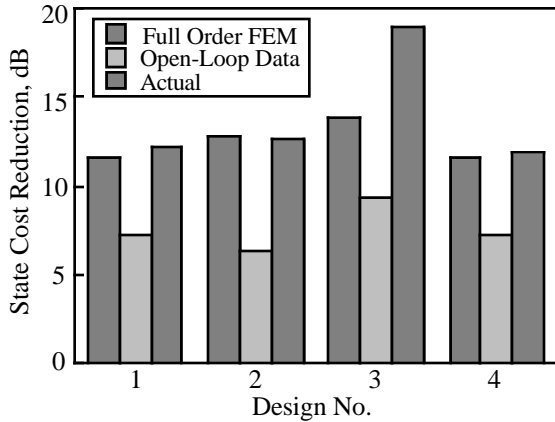

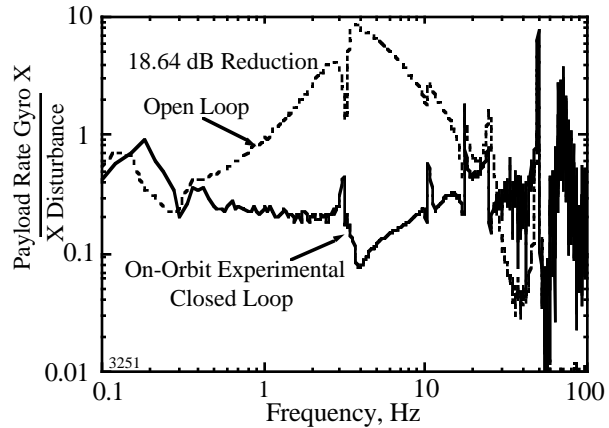Figure 4 SISO X axis control design performance on Configuration 1.

Figure 5 Open-loop vs closed loop performance for a SISO X axis control design on Configuration 1.

Overall, it is seen that the reduction in state cost varied from about 12 to 19 dB. The figure also shows that the actual controller performance was predicted very well by the full order finite element model. Actual performance was notably underpredicted by the open loop data. Since the open loop data was acquired during the first day of testing and the controller evaluations were performed at a later time, it is likely that a slight change in dynamics occurred or that the test article received some type of unscheduled excitation prior to or during acquisition of open loop data. In addition, Design 3 performed much better than Design 1, indicating that notches in the control weighting function resulted in degraded performance.

Figure 5 shows a comparison of the open loop vs. closed loop performance for Design 3 of the SISO X axis controllers. A 19 dB reduction is achieved with a bandwidth of about 25 Hz. In this figure, it is observed that peaks occur in the closed loop transfer function at about 3, 10, and 18 Hz. To determine the source of these peaks, the Nyquist plot and sensitivity diagrams were examined. From the Nyquist diagrams, it was seen that looping occurs near frequencies where the peaks occur in the closed loop transfer function. This indicates inexact cancellation between poles and zeros of the controller and plant. Further, when the sensitivity was examined for this design case, it was seen that robustness violations were predicted at 3, 10 and 20 Hz. The full order FEM predicted the violation at 3Hz. Therefore, the source of peaks in the closed loop transfer function was the combined effect of robustness violations and inexact pole zero cancellation. It is important to note, however, that even with these imperfections, the controller still achieved the overall objective of good disturbance rejection.

Figure 6 shows results from SISO Z axis control design using Configuration 1. The actuator was the primary Z axis gimbal and the sensor was the payload Z axis rate gyro. In

9

these designs, the performance requirement was set at 80% reduction in disturbance levels; the robustness requirement was 5% at low frequencies and 10% at high frequencies; and no noise specification was included. Design 2 is a reduced order version of Design 1, while Design 3 is a reevaluation of Design 1. The secondary Z axis gimbal was used to introduce a 50 Hz bandwidth disturbance during the evaluation of each design.
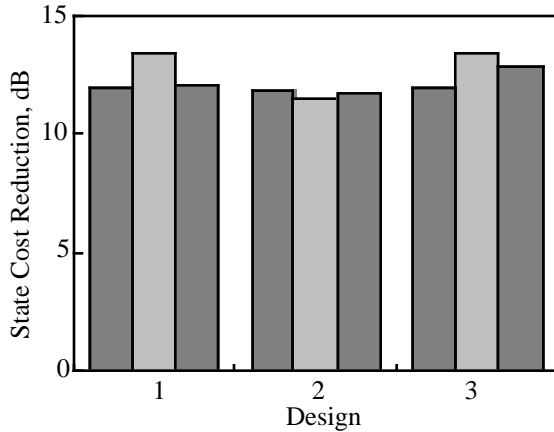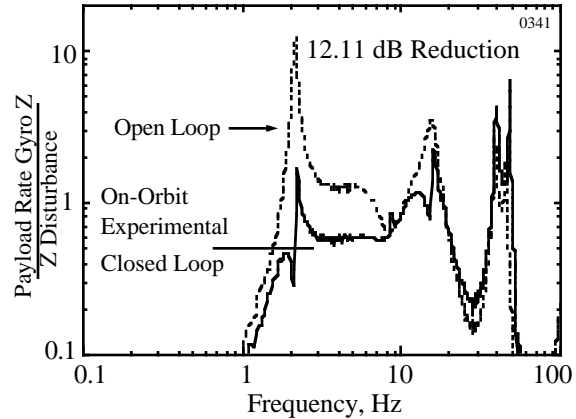
Figure 6 SISO Z axis control design performance on Configuration 1.

Figure 7 Open-loop vs closed loop performance of a SISO Z axis controller for Configuration 1.

The state cost reduction ranged from about 11.5 to 13.5 dB. Both the full order FEM and the open loop data predicted actual results very well. A comparison of the open loop vs. closed loop performance of Design 1 is shown in Figure 7. A 12.11 dB reduction is achieved with a controller bandwidth of about 20 Hz.

SISO Control Design for Configuration 2

Figure 8 shows a comparison of SISO X axis control configurations on Configuration 2. For these designs, the actuator was the primary X axis gimbal and the sensor was the payload X axis rate gyro. The performance requirement for these designs was 20 to 80% reduction of disturbance levels; the robustness requirement was 5% and 10% as before, and no noise requirement was included. Further, variations were made on the control weighting functions and on the design model type (i.e. FEM or MM). The secondary X axis gimbal introduced a 50 Hz bandwidth disturbance.

Reduction in state cost varied from 6 to over 12 dB. In this figure, both the full order FEM and open loop data predict actual performance very well. It is seen, however, that the FEM consistently overpredicts performance by a slight amount, indicating a slight variation in between the FEM predicted dynamics and the dynamics of the test article at the time of testing. Also shown in Figure 8 are Designs 4 and 5 which were developed using a reduced order measurement model (MM) obtained by applying system identification techniques to open loop
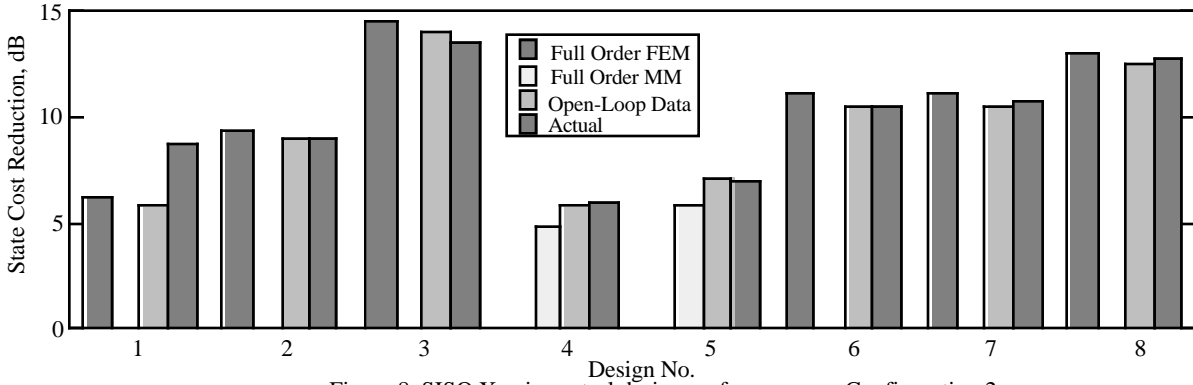
10

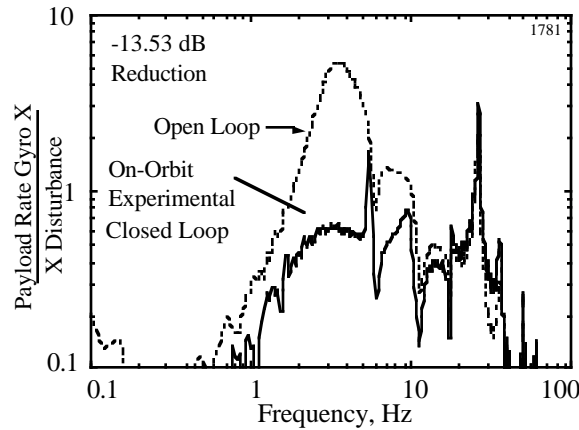Figure 8 SISO X axis control design performance on Configuration 2.

Figure 9 Open-loop vs. closed loop performance for
a SISO X axis control design on Configuration 2.

data obtained on orbit. The performance of these control designs is not as good as designs developed based on the FEM. In fact, Design 5 and Design 6 have identical design specifications but Design 5 was developed using the MM and Design 6 was developed using the FEM. The lower performance of Design 5 implies that the MM did not capture the dynamics of the test article as well as the FEM. This is particularly interesting because the 0-G
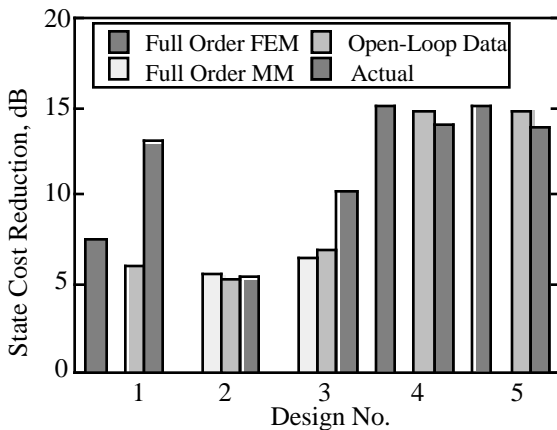

Figure 10 SISO Z axis control design performance
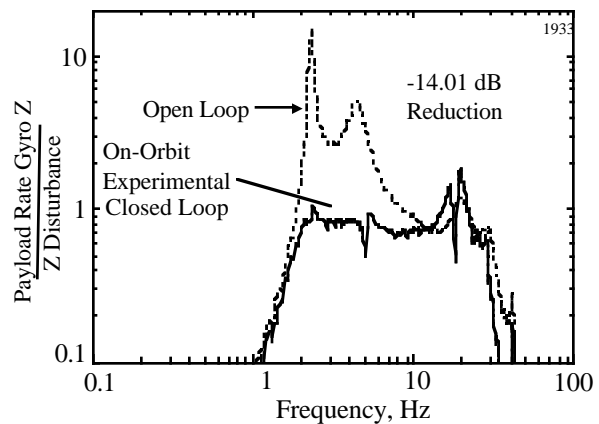on Configuration 2.

Figure 11 Open-loop vs. closed loop performance of a
SISO Z axis control design for Configuration 2.

11

prediction of dynamics by the FEM was groundbased and the MM was developed during the mission using actual data obtained on orbit. A comparison of open loop vs closed loop performance of Design 3 is shown in Figure 9. A 13.5 dB reduction in state cost was achieved and a bandwidth of about 20 Hz.

Figure 10 illustrates a comparison of SISO Z axis control configurations for Configuration 2. The actuator was the primary Z axis gimbal and the sensor was the payload Z axis rate gyro. Design requirements included an 80% reduction in disturbance levels; a 5% and 10% robustness to model uncertainties; and no noise specifications. Variations were made on which design model was used and on the control weighting function. The secondary Z axis gimbal introduced a 50 Hz bandwidth disturbance.

Performance ranged from 5.5 to 14 dB with varied prediction of actual performance by both the FEM and open loop data. Designs 2 and 3 were developed using the MM and, again, show a reduced performance when compared to FEM based designs. A comparison of open loop vs closed loop performance of Design 4 is shown in Figure 11. A 14 dB reduction in state cost was achieved with a bandwidth of above 10 Hz.

Figure 12 illustrates payload disturbance rejection results obtained using Configurations 1 and 2 with X axis reaction wheel actuation and a collocated X axis rate for feedback. Although sensors and actuators at the payload location were not used for control, the performance variable in the H-infinity design procedure was still considered to be output at the payload rate gyro in the X axis. In these two designs, the robustness specification is 5% and 10%, as before, and no noise uncertainty is included. The performance requirement is 20% reduction in disturbance levels for Design 1 and nearly 0% for Design 2. The secondary X axis gimbal introduced a 50 Hz bandwidth disturbance. From the figure, it is seen that the performance achieved was as much as twice what was predicted by either the full order FEM or the open-
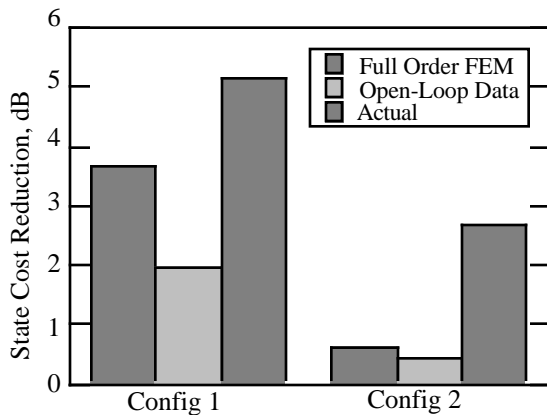

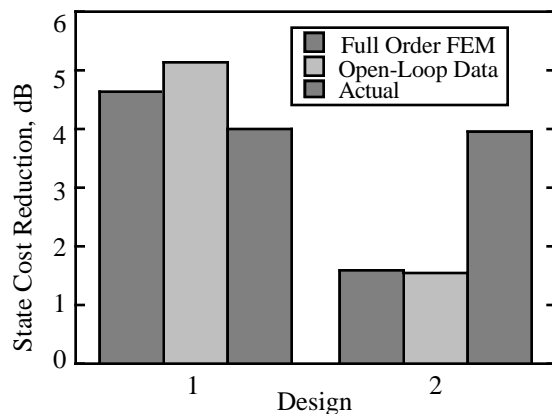Figure 12 SISO X axis control design performance for Reaction Wheel X control only.

Figure 13 SISO Z axis control design performance for Reaction Wheel Z control only on Configuration 2.

loop data, indicating a difference between the design model and actual hardware transfer functions. Reduction achieved was 2.7 to 5.1 dB.

Similar performance levels were obtained on Configuration 2 as shown in Figure 13. For these designs, the performance requirement was 80% reduction in disturbance levels; 5% and10% robustness; and no noise uncertainty. Reduction achieved was about 4 dB. A control weighting variation caused a decrease in the predicted performance of Design 2, although the actual performance remained unaffected. It was concluded, however, that use of the reaction wheels only to isolate the payload from disturbances is not highly effective.

MIMO Control Design

In general, only moderate success was achieved in the evaluation of MIMO designs. One successful design was a MIMO Z axis Configuration 1 controller. Figure 14 illustrates a comparison between the open loop and closed loop performance. In this case, a 13.4 dB reduction in state cost was obtained. Other successes were the MIMO XZ axes control designs. Figure 15 illustrates results for Configuration 1 and 2 experiments. For the implementation of these controllers, two 50 Hz bandwidth disturbances were present simultaneously, one through the secondary Z axis gimbal and the other through the secondary X axis gimbal. The control objective was to reject disturbances from the payload location in the X and Z axis simultaneously. Moderate performance was obtained. About 2.5 to 6.8 dB reduction was obtained in the X axis simultaneous with about 7.5 to 13 dB reduction in the Z axis. These designs had performance specifications of 80% reduction in disturbance levels for the X and Z axes along with a 5% and 10% robustness specification as before and no noise uncertainty.
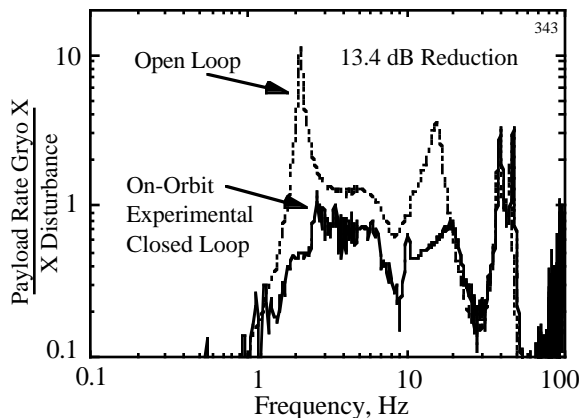

Figure 14   Open-loop vs. closed loop performance of a MIMO Z axis control design on Configuration 1.
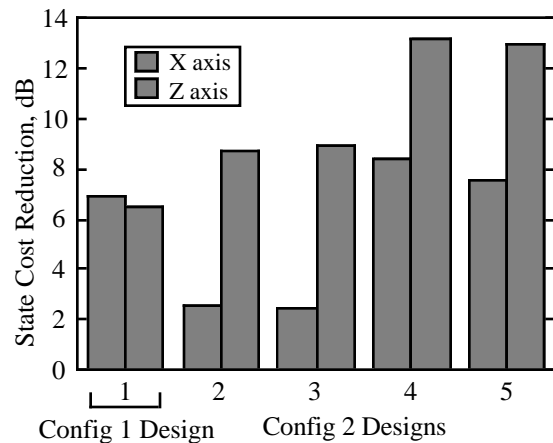

Figure 15   Actual performance of XZ axes control designs for Configurations 1 and 2.

From evaluation of unsuccessful MIMO control designs, several important issues were identified. First, the importance of having accurate information about the hardware control actuation limits, noise levels and other system parameters can not be underestimated. Such knowledge coupled with sufficient experience testing on a laboratory model is critical to making good design decisions and maximizing potential performance of control design. Secondly, not including a multiplicative uncertainty at the plant input may have allowed for increased performance of SISO control designs which tolerated minor robustness violations, but, MIMO designs were much less tolerant of robustness violations. Thus, for MIMO control, guaranteed robustness must be established in the design through the use of a multiplicative uncertainty at the plant input.

Best Design

The best performance obtained during testing was demonstrated by a SISO X axis control design (Figure 5). The 27 state controller demonstrated a state cost reduction of about 19 dB with a bandwidth of over 25 Hz. Although several robustness violations were observed, the performance requirement of reducing the H_∞ norm by 80% was met. The original H_∞ norm was 8.5 over 25 Hz and was reduced by the controller to about 1.8. In fact, over most of the controller bandwidth, the performance requirement was exceeded. When bandwidths up to 20 Hz are considered, the performance improvement was a 94% reduction in disturbance level, with the closed loop H_∞ norm being 0.55 over the frequency range. In regions where robustness violations were not observed, disturbance rejection occurred at even higher levels. This particular design was one which included a multiplicative uncertainty at the plant output to model noise uncertainties. It also contained no notch filters in the control weighting function.

Reduced Order Control Design

Results for the actual performance of full order vs. reduced order controllers are presented in Figure 16. Four SISO designs are presented, one for each of the two configurations and one for each of the two axes of control, X and Z. The original control orders varied from 27 to 34 states. Up to eighteen states were removed from the controller matrices using balanced modal reduction. In all but the first case, the performance between full order and reduced order controllers is nearly the same, indicating the presence of unnecessary dynamics in the full order controllers. The first case shows the performance significantly reduced from 19 dB to 13 dB. From this result, it is apparent that important dynamics were inadvertently removed from the controller during reduction.
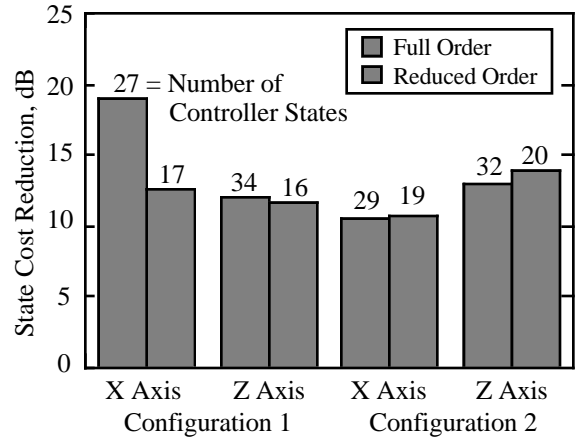
Figure 16 Performance results for reduced
order control designs.

Repeatability

The issue of repeatability of experiments should be addressed. In Figure 4 it is noted that Designs 1 and 4 are identical but were evaluated at different times during the flight experiment. Likewise, in Figure 10, Designs 4 and 5 are identical but evaluated on two separate occasions. In both cases, the actual performance is nearly unchanged, implying that the model dynamics remained relatively unchanged during the flight experiment. Combining this information with the poor prediction of performance by the open loop data shown in Figure 4, it is likely that the test article received some unexpected excitation during or just prior to acquisition of the Configuration 1 open loop data that was used for comparison. The perturbation affected X axis dynamics, whereas, the Z axis dynamics remained unaffected.

CONCLUSIONS

Over 50 H-infinity control designs were experimentally evaluated on the MACE hardware on-orbit. SISO X and Z axis control designs were successfully tested for both hardware Configurations 1 and 2. X axis control designs achieved up to 19 dB reduction in state cost with about 25 Hz bandwidth. Z axis control design achieved up to 14 dB reduction in state cost with up to 20 Hz bandwidth. Several closed loop control systems demonstrated a combined robustness and inexact pole/zero cancellation while maintaining good disturbance rejection. Comparisons of repeated evaluations of X and Z axis SISO controllers at different times during the flight experiment showed that actual performance was nearly unchanged between evaluations. This implied that the model dynamics of interest remained relatively unchanged during the mission. Finally, a comparison between full order and reduced order SISO X and Z axis controllers for both hardware configurations shows nearly identical performance and indicates the presence of unnecessary dynamics in the full order controllers.

MIMO XZ axis control designs were successfully tested on both configurations with moderate performance demonstrated. MIMO designs for Z axis control demonstrated limited success with up to a 13.5 dB reduction, while MIMO X and XY axis control designs were not successful. From evaluation of unsuccessful MIMO control designs, several important issues were identified. First, the importance of having accurate information about the hardware control actuation limits, noise levels and other system parameters is critical to making good design decisions and maximizing potential performance of control design. Secondly, for successful MIMO control, guaranteed robustness must be established in the design through the use of a multiplicative uncertainty at the plant input.

A majority of the control designs tested were designed using the 0-G FEM model developed based on 1-G measurements. This predictive FEM model proved to be excellent. MM based control designs did not perform as well.

The best control design, in terms of performance level achieved, was a SISO X axis design for Configuration 1 which demonstrated a 19 dB reduction in the disturbance level. In addition to the performance and robustness specifications, the H-infinity design structure included a noise uncertainty description and no notches in the control weighting function, both of which seemed to contribute to the superior performance.

Finally, a significant impact of the 0-G environment on control designs was not observed. However, experiments such as MACE serve to demonstrate advanced control technologies and help to promote broader acceptance of these methods with the spacecraft industry.

REFERENCES

[1] LIM, K. B. and COX, D.E, "Robust Tracking Control of a Magnetically Suspended Rigid Body," presented at Second International Symposium on Magnetic Suspension Technology, Seattle, WA, August 11-13, 1993.

[2] BALAS, G. J., and J. C. Doyle, "Control of Lightly Damped, Flexible Modes in the Controller Crossover Region," Journal of Guidance, Control and Dynamics, Vol. 17, No. 2, March-April, 1994.

[3] BALAS, G. J. et al, "μ-Analysis and Synthesis Toolbox: User's Guide," Mathworks, Inc., April, 1991.

[4] GLAESE, R. M. and MILLER, D. W., "Derivation of 0-g Structural Control Models from Analysis and 1-g Experimentation," Proceedings, AIAA Structures, Structural Dynamics and Materials Conference, New Orleans, LA, April, 1995.

[5] LIU, K. and MILLER, D. W., "Time Domain State Space Identification of Structural Systems," submitted to the ASME Journal of Dynamic Systems, Measurement and Control.

[6] MOORE, B. C., "Principal Component Analysis in Linear Systems: Controllability, Observability, and Model Reduction," IEEE Transactions on Automatic Control, Vol. AC-26, No. 1, February, 1981.

[7] GROCOTT, S.C.O., "Comparison of Control Technologies for Robust Performance on Uncertain Structural Systems," Master's Thesis, MIT, 1994.